Influence of anomalous agents on the dynamics of an active system

Nikita P. Kryuchkov,* Artur D. Nasyrov, Konstantin D. Gursky, and Stanislav O. Yurchenko†
Bauman Moscow State Technical University, 2nd Baumanskaya Street 5, 105005 Moscow, Russia

(Received 6 September 2023; accepted 25 January 2024; published 4 March 2024)

Swarming behavior in systems of self-propelled particles, whether biological or artificial, has received increased attention in recent years. Here, we show that even a small number of particles with anomalous behavior can change dramatically collective dynamics of the swarming system and can impose unusual behavior and transitions between dynamic states. Our results pave the way to practical approaches and concepts of multiagent dynamics in groups of flocking animals: birds, insects, and fish, i.e., active and living soft matter.

DOI: 10.1103/PhysRevE.109.034601

I. INTRODUCTION

Natural or artificial active (self-propelled) particles, extensively studied in recent years, manifest a diverse range of phenomena unattainable in equilibrium systems. Examples include motility-induced phase separation [1–6], giant number fluctuations [7–9], active turbulence [10,11], and multistability [12–14]. However, one of the most fascinating features of these systems is their capability of forming various dynamic patterns of collective motions, prominently observed in living systems: collectively moving cells [7,15], insect swarms [16–19], fish schools [20–22], bird flocks [7], and animal herds [23]. The mechanism of swarming behavior varies depending on the system, but it should provide effective attraction and alignment of the moving agents.

The combination of self-propelling and alignment mechanisms is what forms the famous Vicsek model [24], foundational for modern collective motion science. Simple modified Vicsek models allow one to describe diverse collective behaviors, such as fish schooling [22,25,26]. The "swarmalator" system [27], based on the Kuramoto [28] and Vicsek models, introduces the internal parameters for active particles and exhibits sophisticated patterns of dynamic synchronization [29–31]. Moreover, bioinspired swarm algorithms are actively used in complex optimization problems [32] and, potentially, can be applied for decentralized logistics and controlling unmanned vehicles [33]. Finally, in certain cases, people groups behave similarly to simple swarm models [34–36], and this can be used for modeling of public centers to prevent crowding.

The concepts of collective decision making and leadership [37,38] are crucial for understanding diverse swarm behavior phenomena, including those discussed above. In particular, leadership implies the existence of nonreciprocal interactions among agents [39]: as a result, certain agents (leaders) exert a greater influence on the behavior of surrounding agents. To achieve this, specific mechanisms exist within systems: agents can align their behavior with that of older (experienced) [40–42], more dominant [43,44], socially preferred [45], faster [46–48], or signal-emitting agents [15,46,49]. It has been shown [46,50,51] that even a relatively small fraction of leader agents can control the direction of the entire swarm movement. For instance, less than $2-5\%$ of signaling bees (leaders) are sufficient to lead the entire swarm to a new hive [46,51]. However, the question arises, what happens if several agents start behaving differently from the rest but are not perceived as leaders? What influence will they have on the system, and will they be able to alter its dynamic regime? This can occur, for example, if some agents receive additional information but are not recognized by the others as new leaders, or if some agents undergo structural or cognitive disruptions, causing them to no longer behave in the normal manner. Further, we will refer to these agents as *anomalous* to distinguish them from leader agents (where the symmetry of leader-follower interaction is disrupted [39]). However, with a few exceptions [35,50,52,53], the role of such anomalous agents is poorly studied in swarming systems, to our knowledge.

In this paper, we study a fish-school-like system, exhibiting stable swarming, schooling, and milling dynamics. With a method we developed to analyze parameters in the system, we obtained a state diagram and discovered the region of bifurcation behavior, accompanied by sporadic jumping of the system between the pure dynamic states, as well as the regions of dynamic multistability. We further analyze the dynamics in the presence of two kinds of anomalous agents: trying to move horizontally and along circles. We reveal that even 2% of the anomalous agents can impose schooling-milling transitions, thus completely altering the dynamic regimes of the system to a desirable one.

II. MODEL

We studied a monolayer of $N = 100$ self-propelled particles, whose dynamics is described by the equations

$$\begin{aligned} \dot{\boldsymbol{r}}_i &= \mathbf{e}_i^{\parallel}, \\ \dot{\theta}_i &= \langle f_{ij}(\rho_{ij}\sin\theta_{ij} + I_{\parallel}\sin\phi_{ij})\rangle_{V_i} + I_n\eta(t) + A_i, \end{aligned} \tag{1}$$

where $\mathbf{r}_i$ and θ_i are the radius vector and orientation angle of the ith particle, and $\mathbf{e}_i^{\parallel} = (\cos\theta_i, \sin\theta_i)$ is the (unit) velocity vector; the distance ρ_{ij} between the particles i and j, as well

*kruchkov_nkt@mail.ru
†st.yurchenko@mail.ru

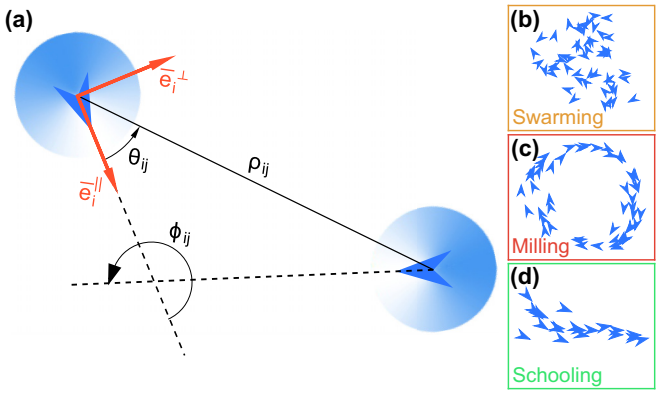

FIG. 1. The model under consideration. (a) A couple of agents with the angles and vectors used in Eq. (1); the gradient circles show the fields of view for oriented particles (triangles). (b)–(d) Swarming, milling, and schooling states.

as the angles θ_{ij} and ϕ_{ij} between their velocities and relative radius, are shown in Fig. 1(a); $f_{ij} = 1/(\rho_{ij} + 1)$ is the cutoff factor (discussed below); $I_\parallel$ and I_n are the magnitudes of particle alignment and noise, respectively; $\eta(t)$ is white Gaussian noise with $\langle \eta(t) \rangle = 0$ and $\langle \eta(t)\eta(t') \rangle = \delta(t - t')$, where δ is Dirac delta function; $\langle \circ \rangle_{V_i} = \sum_{j \in V_i} \circ\, w_{ij} / \sum_{j \in V_i} w_{ij}$ is averaging with weights $w_{ij} = 1 + \cos\theta_{ij}$ (imitating the view field of each particle) over the particles $j \in V_i$ in the neighboring Voronoi cells around the ith particle. A_i in Eq. (1) is the torque we added to introduce anomalous behavior of some particles (i.e., $A_i = 0$ for normal particles).

The model (1) is similar to that proposed in Ref. [22] for a *fish school*, except for some differences: for simplicity, we omitted hydrodynamic interactions [22], introduced the cutoff factor f_{ij} to prevent an artificial linear increase of particle (fish or agents) attraction with distance ρ_{ij}, and replaced the Wiener process with a Gaussian to make the system stationary (otherwise, the rotation of particles begins to accelerate over time). The model (1) is known to have three stable dynamic regimes, sketched in Figs. 1(b)–(d): (i) *swarming*, where the agents move and rotate chaotically within a cluster; (ii) *milling*, where the agents form spinning circlelike structures; and (iii) *schooling*, where the agents are "polarized" and move almost in the same direction. Note that, due to the averaging over Voronoi cells in Eq. (1), agents interact with a small number of neighbors, similar to models with short-range or topological interactions [24,54,55]. At the same time there are models with long-range interactions for swarm dynamics [56–58]. In typical condensed matter systems, it is well known that transition from short- to long-range interactions results in a drastic change in system behavior [59,60]. A similar effect can be expected in the case of swarms. Indeed, considering a larger number of interecting agents leads to the stabilization of new regimes, including turning (see Supplemental Material [61]), which was stabilized by long-range hydrodynamic interactions in the original work [22]. Thus, our results correspond to systems with a small number of interacting neighbors, while the effects of long-range interactions deserve a separate study.

We conducted three sets of simulations, whose parameters are provided in Table I. Here, N_r is the number of independent runs for each combination of parameters. We used Set 1 to obtain the "phase" diagram in the system of identical ($A_i = 0$) particles. Then, to reveal the role of anomalous agents, we selected randomly N_α particles and set a nonzero torque A_i in Eq. (1) for them. We considered two types of anomalous agents: (i) the agents trying to move in the preferred (horizontal) direction $\theta = 0$, that we describe with $A_i = -\alpha\, \mathrm{sgn}(\sin\theta_i) |\sin(\theta_i/2)|$, where $\alpha = 0.02$–0.9 is the magnitude of anomaly (Set 2 in Table I); (ii) the agents trying to move along the circles, that we describe with a constant torque $A_i = \alpha$, $\alpha = 0.04$–0.6 (Set 3 in Table I). Set 2 corresponds to scenarios where anomalous agents intend to move in a particular direction; for instance, a specifically trained sheep leading the rest of the herd in a particular direction [50]. Set 3 corresponds to cases where, for example, an agent, due to physical or cognitive impairments, loses the ability to move straight and constantly turns slightly. In both cases, the parameter α characterizes the force that drives anomalous agents to move in a specific way, compared to the intention of aligning or free will regulated by $I_\parallel$ and I_n, respectively. Note that in the second and third sets of simulations we used variable steps ΔI_n, ΔN_a, and $\Delta\alpha$; see Supplemental Material [61] for details. Each simulation was performed for 1.2×10^5 steps with $\Delta t = 0.01$, where the first 0.2×10^5 steps were used to relax the system (with $A_i = 0$ for all agents), whereas the rest of the steps were used for analysis. At the initial step, the agents had random orientations θ_i and coordinates $\mathbf{r}_i$ uniformly distributed within a square box with an edge $a = 5$. In each new run for the same I_n and $I_\parallel$, the initial positions of the particles did not repeat, and, similarly, the positions of anomalous particles did not repeat when an additional moment A_i was activated (0.2×10^5 steps). By that time, the anomalous particles had "forgotten" their initial positions and were uniformly distributed within the formed swarm (see Supplemental Material [61]). Finally, note that the model we are considering does not have leader-follower asymmetry, making all agents equivalent in this regard.

III. BEHAVIOUR WITHOUT ANOMALOUS AGENTS

For each simulation, we calculated parameters characterizing polarization $P(t)$, milling $M(t)$, and size $S(t)$ of the

TABLE I. Parameters of simulations.

Set no.	Noise I_n	Alignment, $I_\parallel$	Anomalous agents, N_a	Magnitude of anomaly, α	Number of runs, N_r	Total number of runs in the set
1	0–0.95	0–9.5	0		100	40000
2	0.2–0.5	3	1–15	0.02–0.9	50	35100
3	0.1–0.6	8	1–15	0.04–0.6	50	40500

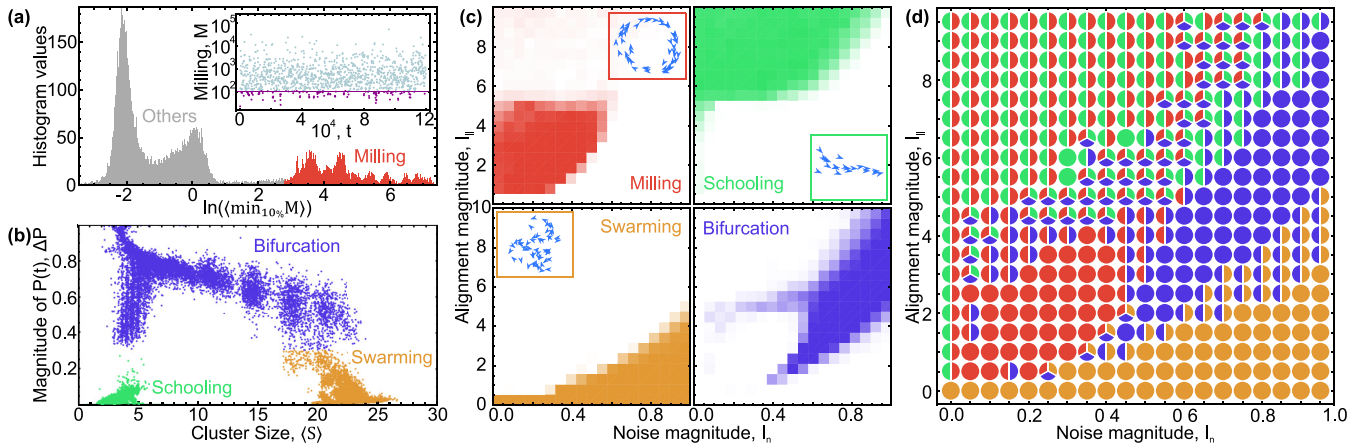

FIG. 2. Dynamic states in the system without anomalous agents ($N_a = 0$, Set 1). (a) The distribution of $\ln(\langle \min_{10\%} M\rangle)$ for all simulations; the red-colored wing corresponds to the milling. The inset shows an example of $M(t)$ in a simulation; 10% of points with minimal M values used to calculate $\ln(\langle \min_{10\%} M\rangle)$ value are colored in magenta. (b) The no-milling states [gray-colored points in (a)] in the plane ΔP vs $\langle S\rangle$, colored in green, orange, and blue for the schooling, swarming, and bifurcation regimes, respectively. (c) Probability distributions of different regimes at different noise and alignment magnitudes I_n and $I_\parallel$. (d) The "phase" diagram of dynamic regimes; colors of each point mark the regimes observed for given magnitudes I_n and $I_\parallel$. The color coding in (c) and (d) is the same as that in (a) and (b).

system:

$$P(t) = |\langle \mathbf{e}_i^{\parallel}\rangle|, \quad M(t) = \frac{\left|\left\langle \mathbf{e}_i^{r} \times \mathbf{e}_i^{\parallel}\right\rangle\right|}{\left|\left\langle \mathbf{e}_i^{r}\right\rangle\right| \cdot \left|\left\langle \mathbf{e}_i^{\parallel}\right\rangle\right|},$$
$$S(t) = \max_i |\mathbf{r}_i - \langle \mathbf{r}_i\rangle|, \quad \mathbf{e}_i^{r} = \frac{\mathbf{r}_i - \langle \mathbf{r}_i\rangle}{|\mathbf{r}_i - \langle \mathbf{r}_i\rangle|}, \tag{2}$$

where $\langle \circ\rangle = \frac{1}{N}\sum_{i=1}^{N} \circ$ denotes averaging over the system. To obtain a "phase" diagram for the studied system, we developed the algorithm based on consistent analysis of $M(t)$, $P(t)$, and $S(t)$ obtained in the simulations.

First, we identified the milling states. We calculated $M(t)$ [a typical example is shown in the inset in Fig. 2(a)] and took a 10% subset of points with minimal M values (magenta colored in the same inset). Then, we averaged the M values over this subset, to obtain $\langle \min_{10\%} M\rangle$. Having done this for all simulations, we summarized the data and obtained the distribution shown for $\ln\langle \min_{10\%} M\rangle$ in Fig. 2(a).

The distribution in Fig. 2(a) splits into two data groups separated by a sizable gap. The right wing (colored in red) corresponds to the milling states; M values here never get too small. Using the gap, we used $\ln(\langle \min_{10\%} M\rangle) > T_*$ with $T_* \simeq 2.8$ as the condition for milling identification. We tested that the threshold T_* can vary within a certain range without a noticeable effect on the following results. Note that as the percentage in $\ln(\langle \min_{10\%} M\rangle)$ increases, approaching 100%, the gap in Fig. 2(a) vanishes. This is because the bifurcation regime combines dynamic states with low and high M values, and corresponding $\ln(\langle \min_{100\%} M\rangle)$ average values fill the gap.

At the second stage, the rest (no-milling) simulations with $\ln(\langle \min_{10\%} M\rangle) < T_*$ were represented in the coordinates ΔP and $\langle S\rangle$, as shown in Fig. 2(b). Here, $\Delta P = \max_t P(t) - \min_t P(t)$ is the magnitude of $P(t)$ fluctuations along the simulation, and $\langle S\rangle$ is the time average for $S(t)$. We see in Fig. 2(b) that the data points become remarkably separated into three groups. The first one, colored green, occupies a region of small ΔP and $\langle S\rangle$, and corresponds to the schooling regime. The groups colored in yellow and blue correspond to the swarming and bifurcation regimes, respectively.

Compared to milling, swarming, or schooling dynamic states, the bifurcation regime is characterized by sporadic "jumping" between them: A certain dynamic state turns out to be short lived: the dynamics of the system is mixed and represents existence in different "pure" states with sporadic jumps between them, that is imprinted in the behavior of M, P, and S parameters. The bifurcation regime becomes very similar to the swarming one under the condition that the frequency of the discussed transitions between different states is sufficiently high. Due to this, the boundary between the bifurcation and swarming regimes in Fig. 2(b) is not so pronounced, compared to that for schooling regime, and we have to choose a threshold $\Delta P = 0.35$ to separate them.

After we identified the dynamic states, we calculated their probabilities at different noise and alignment magnitudes, I_n and $I_\parallel$, the results are shown in Fig. 2(c). The overlapping distributions indicate the presence of multistability, where several stable dynamic states can be observed depending on the initial conditions at the same parameters of the system. The latter is highlighted in Fig. 2(d), wherein the possible states at various I_n and $I_\parallel$ are shown by circles, color coded in the same manner as in Figs. 2(a)–2(c) for milling (red), schooling (green), swarming (yellow), and bifurcation (blue) regimes. Note that multistability is typical for active systems [12–14]. We see in Fig. 2(d) that, in addition to the regions of pure dynamic states, the regions of certain parameters provide bifurcation dynamics, as well as the ability to observe two or three dynamic states.

IV. REVEALING THE ROLE OF ANOMALOUS AGENTS

We discovered that anomalous agents can change dynamic states and impose the milling-schooling or schooling-milling

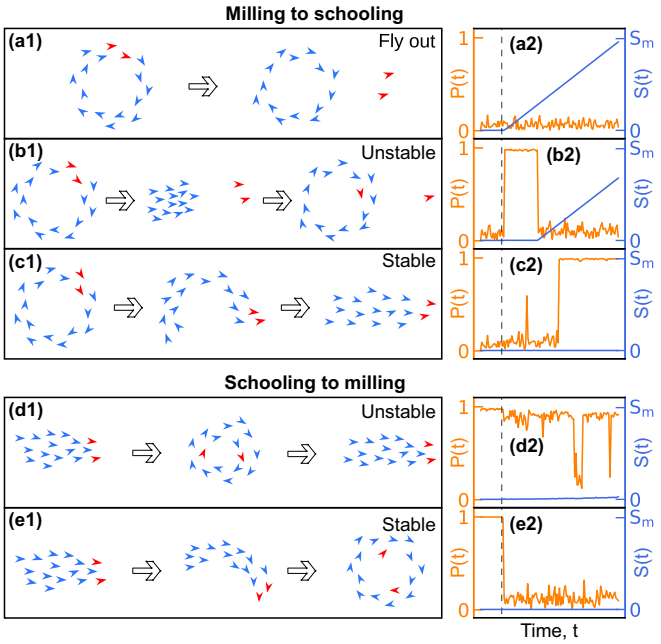

FIG. 3. Dynamics in the presence of anomalous agents. (a1)–(e1) Sketches of configurations and transitions between them; anomalous agents are shown with red arrows. (a2)–(e2) corresponding dependencies $P(t)$ and $S(t)$, colored in orange and blue, respectively. The vertical black dashed lines indicate the start of anomalous particle action.

transitions. Various scenarios we observed are illustrated in Fig. 3: Here, Figs. 3(a1)–3(c1) correspond to Set 2 with anomalous particles trying to move horizontally, whereas the results for Set 3 with anomalous particles trying to move through circles are shown in Figs. 3(d1) and 3(e1). Corresponding evolution of $P(t)$ and $S(t)$ is shown in Figs. 3(a2)–3(e2). Probability distributions for different scenarios we discuss below are presented in Figs. 4(a) and 4(b) for Sets 2 and 3, respectively. System states are depicted in sketches in Figs. 3 for simplicity; simulation snapshots of the system can be found in the Supplemental Material [61].

In the case of the anomalous agents tryin to move in a preferred direction (Set 2), we observed four scenarios. At small N_a and α, there no noticeable effect was observed. At $N_a \lesssim 2$ and large α, we observed another scenario: The anomalous agents were flying out from the cluster, leaving it in the initial dynamic state, as shown in Fig. 3(a). Such cases are characterized by small $P(t)$ and growing $S(t)$ with $dS/dt \approx 1$. An increase in the noise magnitude I_n suppresses this effect, shifting it to higher α, as seen in Figs. 4(a1)–4(a6).

In the third scenario, shown in Fig. 3(b) (two-step transition), the system first undergoes a transition from milling to schooling state and then returns back to the milling one, that is accompanied by a synchronous change in $P(t)$. Corresponding probabilities for various I_n are shown Figs. 4(a7)–4(a12). This behavior is practically always observed at high magnitudes $I_n \gtrsim 0.38$, except for a narrow yellow-colored region in Fig. 4(a7), where the system undergoes a stable milling-schooling transition, the fourth dynamic scenario we observed.

The yellow region in Fig. 4(a7) separates behaviors of the system. At the top of the region, we observe transitions to schooling, whereas the anomalous agents are ahead and move on average faster than the rest of the particles, due to smaller dispersion in θ. As a result, after a while, the anomalous particles go ahead far enough that the rest of the particles lose sight of them and return to their normal regime (milling). Therefore, the milling-schooling transition observed in this region is unstable over the long term, but it can be stabilized by reducing the speed of the anomalous agents. Under the

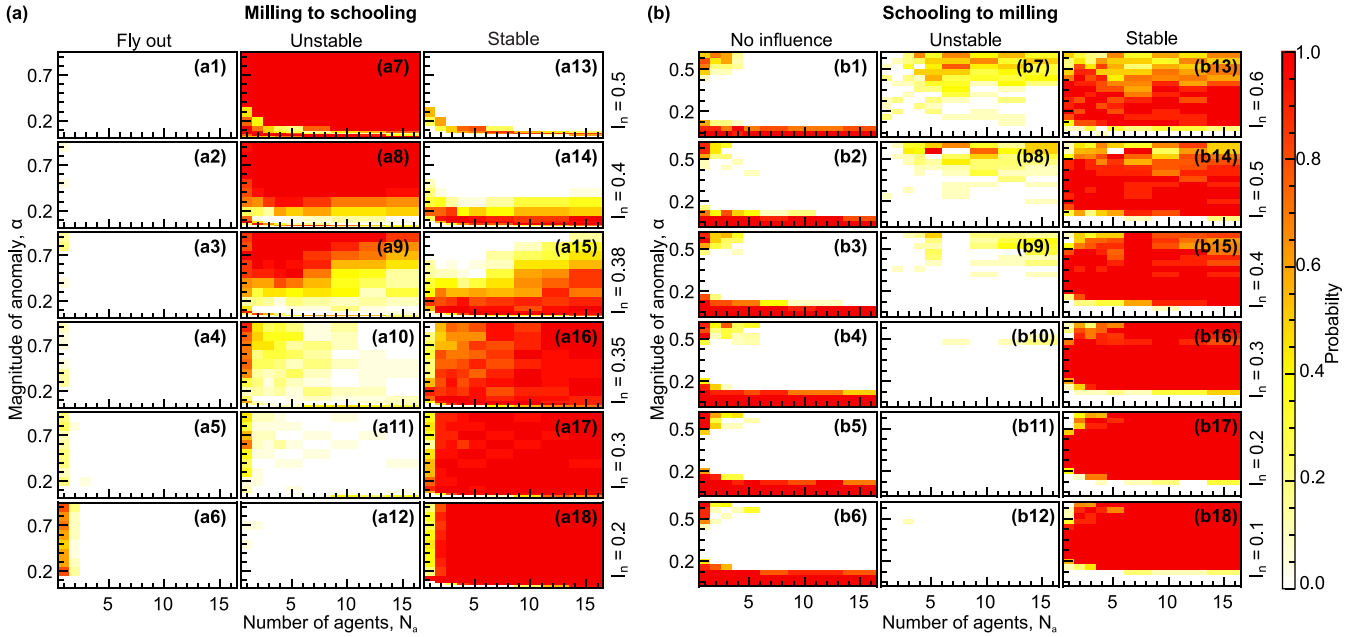

FIG. 4. Probability distribution functions for the formation of a specific dynamic scenario in the systems with anomalous agents: (a) and (b) illustrate the results for Sets 2 and 3, wherein anomalous agents induce milling-schooling or schooling-milling transitions, respectively.

yellow region in Fig. 4(a7), the schooling regime is unstable and switches sporadically. The distributions in Fig. 4(a) change dramatically at $I_n < 0.38$. The region of the unstable scenario shown in Fig. 3(b1) becomes rapidly shifted towards large α. At the same time, the stable scenario illustrated in Fig. 3(c) starts to prevail, as depicted in Figs. 4(a16)–4(a18).

Note that the state with $I_n = 0.5$ from Set 2 falls within the region where both milling and bifurcation regimes can occur, as shown in Fig. 2(d). However, according to Fig. 2(c), the probability of the bifurcation regime is low. Nevertheless, we suppose that if a bifurcation regime were to be realized in this case, the presence of anomalous particles would more strongly bias the bifurcation regime into a schooling regime, stabilizing it.

Finally, we observed only three scenarios in simulation Set 3: (i) the regime does not change, (ii) there are random jumps of the system between two states, and (iii) there are transitions between schooling and milling regimes induced by anomalous particles. All these cases are imprinted in the behavior of $P(t)$ shown in Figs. 3(d2) and 3(e2). Corresponding distributions are shown in Fig. 4(b), and are practically independent of N_a. The schooling regime is stable at small α (until the anomaly is too weak) and at large α. In the latter case, the anomalous agents are forced to rotate in place, and are frozen and fall behind the entire system. The range of intermediate α corresponds to a stable schooling-milling transition, while two-step behavior is observed at larger magnitudes I_n. Without anomalous agents, milling or schooling states can exist under the parameters of simulation Set 3. Therefore, without a noise-induced rebound to the initial state, the system lives for a long time in the induced one, which explains such a large area of the stable scenario. This is a reason for prevalence of the stable scenario at intermediate α values. The transitions between milling and schooling can be induced even by one particle, under appropriate α and I_n. However, at small I_n, a single anomalous agent will most likely leave the cluster before the change in collective dynamics.

Our results coincide with the previous studies on analogous systems featuring anomalous agents. For instance, it was demonstrated [50] that even 5–10% of anomalous agents (where the symmetry of leader-follower interaction is not broken) are sufficient to control the direction of swarm movement. In another study [52], it was experimentally shown that a specially trained sheep, which we can consider as an anomalous agent, can initiate movement and lead a flock of up to 100 sheep in the desired direction. It is interesting that they observed a trained sheep (an anomalous agent) being able to leave the rest of the herd without altering its dynamics, which corresponds to the fly-out regime observed in our study. Similarly, a change in the dynamic regime due to anomalous agents was observed in the simulation of the movement of a large group of people [35], but under confinement conditions and with a significantly higher concentration of anomalous agents.

V. CONCLUSION

We studied a two-dimensional fish-school-like system and revealed the possible role of anomalous agents. For a system without anomalous agents, we obtained a "phase" diagram including milling, schooling, swarming, and bifurcation dynamics. Moreover, we showed an inherent multistability of the system and revealed the regions of bifurcation dynamic behavior. We found that even a small part of anomalous agents can change collective dynamics: Even 2% of anomalous particles can trigger milling-schooling transition. In the case of fish, even such a tiny part of fish assistants can save the whole shoal from a disaster by changing its motion.

Our results raise a number of issues, related to the size effect, the role of interparticle interactions, the capability to control the collective dynamics in three-dimensional systems, and the initial position of anomalous particles on the transition. The method we developed to obtain "phase" diagrams of active systems can be applied to other ones. We leave corresponding studies for future works.

The results should be of interest to a broad community in active and living soft matter, nonlinear dynamics, and collective behavior. In particular, the discovered role of anomalous particles offers ideas for future approaches to ecological regulation for animal husbandry, fishing, migration balancing, and reducing damage to wildlife in environmental disasters.

ACKNOWLEDGMENT

The study was supported by the Russian Science Foundation, Grant No. 20-72-10161.

N.P.K. conceived and directed the research and performed simulations; N.P.K., A.D.N., and K.D.G. processed simulations; N.P.K., A.D.N., K.D.G., and S.O.Y. analyzed and discussed the results; N.P.K. and S.O.Y. wrote the manuscript. All authors reviewed the manuscript.

[1] I. Buttinoni, J. Bialké, F. Kümmel, H. Löwen, C. Bechinger, and T. Speck, Dynamical clustering and phase separation in suspensions of self-propelled colloidal particles, Phys. Rev. Lett. **110**, 238301 (2013).

[2] M. E. Cates and J. Tailleur, Motility-induced phase separation, Annu. Rev. Condens. Matter Phys. **6**, 219 (2015).

[3] S. Mandal, B. Liebchen, and H. Löwen, Motility-induced temperature difference in coexisting phases, Phys. Rev. Lett. **123**, 228001 (2019).

[4] G. S. Redner, M. F. Hagan, and A. Baskaran, Structure and dynamics of a phase-separating active colloidal fluid, Phys. Rev. Lett. **110**, 055701 (2013).

[5] J. Bickmann and R. Wittkowski, Predictive local field theory for interacting active Brownian spheres in two spatial dimensions, J. Phys.: Condens. Matter **32**, 214001 (2020).

[6] N. P. Kryuchkov, A. D. Nasyrov, K. D. Gursky, and S. O. Yurchenko, Inertia changes evolution of motility-induced phase separation in active matter across particle activity, Phys. Rev. E **107**, 044601 (2023).

[7] T. Vicsek and A. Zafeiris, Collective motion, Phys. Rep. **517**, 71 (2012).
[8] V. Narayan, S. Ramaswamy, and N. Menon, Long-lived giant number fluctuations in a swarming granular nematic, Science **317**, 105 (2007).
[9] S. Dey, D. Das, and R. Rajesh, Spatial structures and giant number fluctuations in models of active matter, Phys. Rev. Lett. **108**, 238001 (2012).
[10] R. Großmann, P. Romanczuk, M. Bär, and L. Schimansky-Geier, Vortex arrays and mesoscale turbulence of self-propelled particles, Phys. Rev. Lett. **113**, 258104 (2014).
[11] N. P. Kryuchkov and S. O. Yurchenko, Collective excitations in active fluids: Microflows and breakdown in spectral equipartition of kinetic energy, J. Chem. Phys. **155**, 024902 (2021).
[12] N. P. Kryuchkov, L. A. Mistryukova, A. V. Sapelkin, and S. O. Yurchenko, Strange attractors induced by melting in systems with nonreciprocal effective interactions, Phys. Rev. E **101**, 063205 (2020).
[13] N. P. Kryuchkov, A. V. Ivlev, and S. O. Yurchenko, Dissipative phase transitions in systems with nonreciprocal effective interactions, Soft Matter **14**, 9720 (2018).
[14] G. Gogia and J. C. Burton, Emergent bistability and switching in a nonequilibrium crystal, Phys. Rev. Lett. **119**, 178004 (2017).
[15] R. Mayor and S. Etienne-Manneville, The front and rear of collective cell migration, Nat. Rev. Mol. Cell Biol. **17**, 97 (2016).
[16] J. Buhl, D. J. T. Sumpter, I. D. Couzin, J. J. Hale, E. Despland, E. R. Miller, and S. J. Simpson, From disorder to order in marching locusts, Science **312**, 1402 (2006).
[17] J. E. Ron, I. Pinkoviezky, E. Fonio, O. Feinerman, and N. S. Gov, Bi-stability in cooperative transport by ants in the presence of obstacles, PLoS Comput. Biol. **14**, e1006068 (2018).
[18] O. Feinerman, I. Pinkoviezky, A. Gelblum, E. Fonio, and N. S. Gov, The physics of cooperative transport in groups of ants, Nat. Phys. **14**, 683 (2018).
[19] G. Ariel and A. Ayali, Locust collective motion and its modeling, PLoS Comput. Biol. **11**, e1004522 (2015).
[20] K. Tunstrøm, Y. Katz, C. C. Ioannou, C. Huepe, M. J. Lutz, and I. D. Couzin, Collective states, multistability and transitional behavior in schooling fish, PLoS Comput. Biol. **9**, e1002915 (2013).
[21] D. S. Calovi, U. Lopez, S. Ngo, C. Sire, H. Chaté, and G. Theraulaz, Swarming, schooling, milling: Phase diagram of a data-driven fish school model, New J. Phys. **16**, 015026 (2014).
[22] A. Filella, F. Nadal, C. Sire, E. Kanso, and C. Eloy, Model of collective fish behavior with hydrodynamic interactions, Phys. Rev. Lett. **120**, 198101 (2018).
[23] F. Ginelli, F. Peruani, M.-H. Pillot, H. Chaté, G. Theraulaz, and R. Bon, Intermittent collective dynamics emerge from conflicting imperatives in sheep herds, Proc. Natl. Acad. Sci. USA **112**, 12729 (2015).
[24] T. Vicsek, A. Czirók, E. Ben-Jacob, I. Cohen, and O. Shochet, Novel type of phase transition in a system of self-driven particles, Phys. Rev. Lett. **75**, 1226 (1995).
[25] M. Jiang, A. Zhou, R. Chen, Y. Yang, H. Dong, and W. Wang, Collective motions of fish originate from balanced local perceptual interactions and individual stochastics, Phys. Rev. E **107**, 024411 (2023).
[26] D. Liu, Y. Liang, J. Deng, and W. Zhang, Modeling three-dimensional bait ball collective motion, Phys. Rev. E **107**, 014606 (2023).
[27] K. P. O'Keeffe, H. Hong, and S. H. Strogatz, Oscillators that sync and swarm, Nat. Commun. **8**, 1504 (2017).
[28] J. A. Acebrón, L. L. Bonilla, C. J. Pérez Vicente, F. Ritort, and R. Spigler, The kuramoto model: A simple paradigm for synchronization phenomena, Rev. Mod. Phys. **77**, 137 (2005).
[29] T. A. McLennan-Smith, D. O. Roberts, and H. S. Sidhu, Emergent behavior in an adversarial synchronization and swarming model, Phys. Rev. E **102**, 032607 (2020).
[30] S. Ceron, K. O'Keeffe, and K. Petersen, Diverse behaviors in non-uniform chiral and non-chiral swarmalators, Nat. Commun. **14**, 940 (2023).
[31] G. K. Sar, S. N. Chowdhury, M. Perc, and D. Ghosh, Swarmalators under competitive time-varying phase interactions, New J. Phys. **24**, 043004 (2022).
[32] M. N. A. Wahab, S. Nefti-Meziani, and A. Atyabi, A comprehensive review of swarm optimization algorithms, PLoS ONE **10**, e0122827 (2015).
[33] J. D. Monaco, G. M. Hwang, K. M. Schultz, and K. Zhang, Cognitive swarming in complex environments with attractor dynamics and oscillatory computing, Biol. Cybern. **114**, 269 (2020).
[34] J. L. Silverberg, M. Bierbaum, J. P. Sethna, and I. Cohen, Collective motion of humans in mosh and circle pits at heavy metal concerts, Phys. Rev. Lett. **110**, 228701 (2013).
[35] A. Kulkarni, S. P. Thampi, and M. V. Panchagnula, Sparse game changers restore collective motion in panicked human crowds, Phys. Rev. Lett. **122**, 048002 (2019).
[36] I. Karamouzas, B. Skinner, and S. J. Guy, Universal power law governing pedestrian interactions, Phys. Rev. Lett. **113**, 238701 (2014).
[37] A. J. King and C. Sueur, Where next? Group coordination and collective decision making by primates, Int. J. Primatol. **32**, 1245 (2011).
[38] L. Conradt and T. J. Roper, Group decision-making in animals, Nature (London) **421**, 155 (2003).
[39] J. Garland, A. M. Berdahl, J. Sun, and E. M. Bollt, Anatomy of leadership in collective behaviour, Chaos **28**, 075308 (2018).
[40] C. J. Torney, M. Lamont, L. Debell, R. J. Angohiatok, L.-M. Leclerc, and A. M. Berdahl, Inferring the rules of social interaction in migrating caribou, Philos. Trans. R. Soc. B **373**, 20170385 (2018).
[41] K. McComb, G. Shannon, S. M. Durant, K. Sayialel, R. Slotow, J. Poole, and C. Moss, Leadership in elephants: The adaptive value of age, Proc. R. Soc. B **278**, 3270 (2011).
[42] L. J. Brent, D. W. Franks, E. A. Foster, K. C. Balcomb, M. A. Cant, and D. P. Croft, Ecological knowledge, leadership, and the evolution of menopause in killer whales, Curr. Biol. **25**, 746 (2015).
[43] A. J. King, C. M. Douglas, E. Huchard, N. J. Isaac, and G. Cowlishaw, Dominance and affiliation mediate despotism in a social primate, Curr. Biol. **18**, 1833 (2008).
[44] R. O. Peterson, A. K. Jacobs, T. D. Drummer, L. D. Mech, and D. W. Smith, Leadership behavior in relation to dominance and reproductive status in gray wolves, canis lupus, Can. J. Zool. **80**, 1405 (2002).

[45] N. W. Bode, A. J. Wood, and D. W. Franks, The impact of social networks on animal collective motion, Anim. Behav. **82**, 29 (2011).

[46] R. C. Fetecau and A. Guo, A mathematical model for flight guidance in honeybee swarms, Bull. Math. Biol. **74**, 2600 (2012).

[47] B. Pettit, Z. Akos, T. Vicsek, and D. Biro, Speed determines leadership and leadership determines learning during pigeon flocking, Curr. Biol. **25**, 3132 (2015).

[48] B. Pettit, A. Perna, D. Biro, and D. J. T. Sumpter, Interaction rules underlying group decisions in homing pigeons, J. R. Soc. Interface **10**, 20130529 (2013).

[49] A. Attanasi, A. Cavagna, L. Del Castello, I. Giardina, A. Jelic, S. Melillo, L. Parisi, O. Pohl, E. Shen, and M. Viale, Emergence of collective changes in travel direction of starling flocks from individual birds' fluctuations, J. R. Soc. Interface **12**, 20150319 (2015).

[50] I. D. Couzin, J. Krause, N. R. Franks, and S. A. Levin, Effective leadership and decision-making in animal groups on the move, Nature (London) **433**, 513 (2005).

[51] T. D. Seeley, *Honeybee Ecology* (Princeton University Press, Princeton, 1985).

[52] S. Toulet, J. Gautrais, R. Bon, and F. Peruani, Imitation combined with a characteristic stimulus duration results in robust collective decision-making, PLoS ONE **10**, e0140188 (2015).

[53] G. K. Sar, D. Ghosh, and K. O'Keeffe, Pinning in a system of swarmalators, Phys. Rev. E **107**, 024215 (2023).

[54] V. Dossetti, F. J. Sevilla, and V. M. Kenkre, Phase transitions induced by complex nonlinear noise in a system of self-propelled agents, Phys. Rev. E **79**, 051115 (2009).

[55] E. Cristiani, M. Menci, M. Papi, and L. Brafman, An all-leader agent-based model for turning and flocking birds, J. Math. Biol. **83**, 45 (2021).

[56] M. Zumaya, H. Larralde, and M. Aldana, Delay in the dispersal of flocks moving in unbounded space using long-range interactions, Sci. Rep. **8**, 15872 (2018).

[57] D. J. G. Pearce, A. M. Miller, G. Rowlands, and M. S. Turner, Role of projection in the control of bird flocks, Proc. Natl. Acad. Sci. USA **111**, 10422 (2014).

[58] A. Cavagna and I. Giardina, Bird flocks as condensed matter, Annu. Rev. Condens. Matter Phys. **5**, 183 (2014).

[59] S. C. Kapfer and W. Krauth, Two-dimensional melting: From liquid-hexatic coexistence to continuous transitions, Phys. Rev. Lett. **114**, 035702 (2015).

[60] E. Luijten and H. W. J. Blöte, Boundary between long-range and short-range critical behavior in systems with algebraic interactions, Phys. Rev. Lett. **89**, 025703 (2002).

[61] See Supplemental Material at http://link.aps.org/supplemental/10.1103/PhysRevE.109.034601 for extended simmulatin details and additional snapshots.